Front. Agr. Sci. Eng. 2017, **4**(1): 116–120
DOI: 10.15302/J-FASE-2017141
Available online at http://engineering.cae.cn

RESEARCH ARTICLE

Synthesis of $MnFe_2O_4$/cellulose aerogel nanocomposite with strong magnetic responsiveness

Jian LI (✉), Yue JIAO, Caichao WAN

Material Science and Engineering College, Northeast Forestry University, Harbin 150040, China

Abstract Cellulose aerogel, with abundant three-dimensional architecture, has been considered as a class of ideal eco-friendly matrix materials to encapsulate various nanoparticles for synthesis of miscellaneous functional materials. In the present paper, hexagonal single-crystalline $MnFe_2O_4$ was fabricated and inserted into the cellulose aerogel using an *in situ* chemical precipitation method. The as-prepared $MnFe_2O_4$ nanoparticles were well dispersed and immobilized in the micro/nanoscale pore structure of the aerogel, and exhibited superparamagnetic behavior. In addition, the nanocomposite was easily actuated under the effect of an external magnetic field, revealing its strong magnetic responsiveness. Combined with the advantages of environmental benefits, facile synthesis method, strong magnetic responsiveness, and unique structural feature, this class of $MnFe_2O_4$/cellulose aerogel nanocomposite has possible uses for applications such as magnetically actuated adsorbents.

Keywords cellulose aerogel, $MnFe_2O_4$, magnetic responsiveness, nanocomposite

1 Introduction

Aerogel based on cellulose, the most abundant and renewable natural polymer, is considered as one of the most promising cellulose products. Cellulose aerogel consists of a cross-linked three-dimensional (3D) network. The unique structural characteristic endows itself with low density, high porosity and large specific surface area[1–3]. As a result, cellulose aerogel finds applications in multitudinous fields such as adsorbing materials[4], catalyst supports[5], and super-thermal and sound insulators[6]. In recent years, cellulose aerogel has gained increasing attention for magnetic devices. Magnetic cellulose aerogel is a kind of cellulose aerogel which shows magnetic responsiveness under the action of an additional magnetic field. In general, magnetic nanoparticles (e.g., α-FeOOH, $CoFe_2O_4$, Fe_2O_3, Fe_3O_4 and $MnFe_2O_4$) are loaded in the aerogel in order to endow magnetic properties, and the resultant magnetic aerogel has diamagnetic, paramagnetic, ferromagnetic, ferrimagnetic or antiferromagnetic characteristics[7,8], mainly dependent on the inserted magnetic nanoparticles. Chin et al. prepared magnetic cellulose aerogel by *in situ* incorporation of magnetic Fe_3O_4 nanoparticles into the cellulose aerogel[9]. The hybrid aerogel can be easily recovered from water by applying an external magnetic field. Liu et al. obtained magnetic $CoFe_2O_4$/cellulose hybrid aerogel by using cellulose aerogel as a template, and the formed magnetic composite aerogel was lightweight, flexible, and highly porous[10]. Wan and Li prepared superparamagnetic γ-Fe_2O_3 nanoparticles encapsulated in 3D architecture of cellulose aerogel for the application of removing Cr^{6+} ions from contaminated water[11]. Based on these reports, it was found that the magnetic composite aerogel not only had strong magnetic responsiveness, but also the unique physicochemical properties of cellulose aerogel. These multifarious functions contribute to expanding the scope of its potential application.

$MnFe_2O_4$ is a typical soft ferrite with a small magnetic anisotropy constant of about 10^3 $J \cdot m^{-3}$[12]. $MnFe_2O_4$ nanoparticles have attracted considerable attention because of their potential as contrast enhancement agents in magnetic resonance imaging technology[13,14]. It is well-known that nanoparticles readily agglomerate due to high surface energy, which leads to performance deterioration. Therefore, integration of magnetic nanoparticles, such as $MnFe_2O_4$, within a porous substrate, such as cellulose aerogel, might not only provide magnetically actuated aerogel, but also effectively reduce the particle agglomeration.

Received December 15, 2016; accepted January 14, 2017

Correspondence: nefulijian@163.com

In the present study, hexagonal single-crystalline $MnFe_2O_4$ was fabricated and inserted into the cellulose aerogel using an *in situ* chemical precipitation method. The morphology, crystal structure, chemical components and thermodynamic stability of the as-prepared $MnFe_2O_4$/cellulose aerogel (coded as $MnFe_2O_4$/CA) nanocomposite were investigated by scanning electron microscopy (SEM), energy-dispersive X-ray (EDX), transmission electron microscopy (TEM), selected area electron diffraction (SAED), X-ray diffraction (XRD), thermogravimetric (TG) analysis and X-ray photoelectron spectroscopy (XPS). The magnetic properties of the nanocomposite was also tested by superconducting quantum interference device.

2 Materials and methods

2.1 Materials

Chemical reagents including $FeSO_4 \cdot 7H_2O$, KNO_3, $MnCl_2 \cdot 4H_2O$, and NaOH were of analytical grade and purchased from Tianjin Kemiou Chemical Reagent Co., Ltd. (Tianjin, China) and used without further purification.

2.2 Preparation of $MnFe_2O_4$/CA

The preparation process of cellulose hydrogel (the precursor of cellulose aerogel) was described in previous reports[15,16]. The prepared cellulose hydrogel was immersed in a freshly prepared aqueous solution of $FeSO_4 \cdot 7H_2O$ and $MnCl_2 \cdot 4H_2O$ (40 mL) with the stoichiometric ratio of Mn:Fe of 1:2. After 1 h of immersion, the mixture was heated to 90°C and held at this temperature for 2 h. KNO_3 and NaOH were dissolved in 40 mL of distilled water. This solution was heated to 90°C, and quickly added to the suspension of metal ions/cellulose hydrogel. The molar ratios of $[Mn^{2+}]$:$[OH^-]$ and $[Mn^{2+}]$:$[KNO_3]$ were 1:2 and 1:3, respectively. The mixed system was kept for an additional 6 h at 90°C. All reactions were performed in air. The resulting product was washed repeatedly with distilled water and tert-butyl alcohol to remove residual chemicals, and then underwent a tert-butyl alcohol freeze-drying treatment at −35°C for 24 h. In addition, the pure cellulose aerogel was prepared by the tert-butyl alcohol freeze-drying treatment of the cellulose hydrogel.

2.3 Characterization

The morphology was observed by SEM (FEI, Quanta 200) equipped with an EDX spectrometer for elemental analysis. TEM and high-resolution TEM (HRTEM) observations and SAED were performed with a FEI, Tecnai G2 F20 TEM with a field-emission gun operating at 200 kV. XRD was implemented on a Bruker D8 Advance TXS XRD instrument. XPS was carried out using a Thermo Escalab 250Xi XPS spectrometer equipped with a dual X-ray source using Al Kα. Thermal stabilities were determined using a TG analyzer (TA, Q600) from room temperature to 800°C at a heating rate of $10°C \cdot min^{-1}$ under a nitrogen atmosphere. A magnetometer (MPMS XL-7, Quantum Design) using a superconducting quantum interference device sensor was used to make a measurement of the magnetic properties of the nanocomposite in applied magnetic fields over the range from −20000 to + 20000 Oe at 298 K.

3 Results and discussion

The SEM image demonstrates that $MnFe_2O_4$/CA maintained a 3D interconnected network after the incorporation of $MnFe_2O_4$ (Fig. 1a). However, it is difficult to distinguish the $MnFe_2O_4$ nanoparticles from the complicated network structure. Even the higher-magnification SEM image still cannot identify the nanoparticles (Fig. 1b), possibly due to their extremely small particle size. The following TEM observation confirmed this. Compared with the pure cellulose aerogel, apart from the common C and O, the EDX spectrum of $MnFe_2O_4$/CA exhibited new peaks assigned to S, K, Fe and Mn (Fig. 1c). The Fe and Mn originated from the synthetic $MnFe_2O_4$, while the S and K are attributed to the residual chemicals. Further insight into the microstructure of the $MnFe_2O_4$ in the cellulose aerogel was gained by using TEM and HRTEM. It can be seen in Fig. 1d that the nanoparticles (the dark spots of hexagon) with the sizes ranging from 70 to 140 nm were homogeneously dispersed and immobilized in the cellulose aerogel matrix, which indicates that the cellulose aerogel with 3D architecture is a suitable template for the synthesis of nanoparticles. The SAED pattern was obtained on an individual $MnFe_2O_4$ nanoparticle, as shown in Fig. 1e. It clearly demonstrates that the hexagonal $MnFe_2O_4$ was essentially a single crystalline structure. Figure 1f presents the HRTEM image of the hexagonal $MnFe_2O_4$. The lattice spacing between two adjacent fringes was 0.26 nm, corresponding to the (311) plane of $MnFe_2O_4$.

For clarifying the crystal structure and phase purity of the synthesized particles, XRD analysis was conducted. As shown in Fig. 2, the characteristic peaks of cellulose can be observed at 12.3°, 20.2° and 22.0° for both the cellulose aerogel and $MnFe_2O_4$/CA, corresponding to $(\bar{1}10)$, (110) and (200) planes[17], respectively. Also, the peaks of $MnFe_2O_4$/CA at 29.7°, 34.9°, 42.5°, 52.7°, 56.2° and 61.6° are related to (220), (311), (400), (422), (511) and (440), respectively, according to the Joint Committee on Powder Diffraction Standards file of $MnFe_2O_4$ (No. 10-0319). This analysis indicates the formation of $MnFe_2O_4$ with a spinel ferrite crystalline structure. In addition, there is no

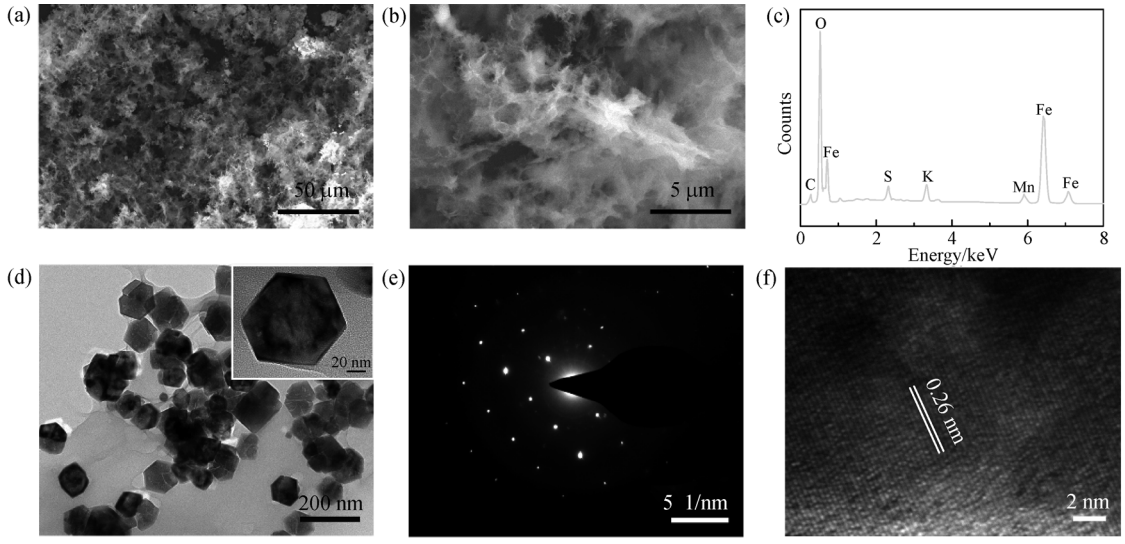

Fig. 1 SEM images (a, b), EDX pattern (c), TEM image (d), SAED pattern (e), and HRTEM image (f) of $MnFe_2O_4$/CA, respectively. The inset in (d) shows the shape of single $MnFe_2O_4$ nanoparticle.

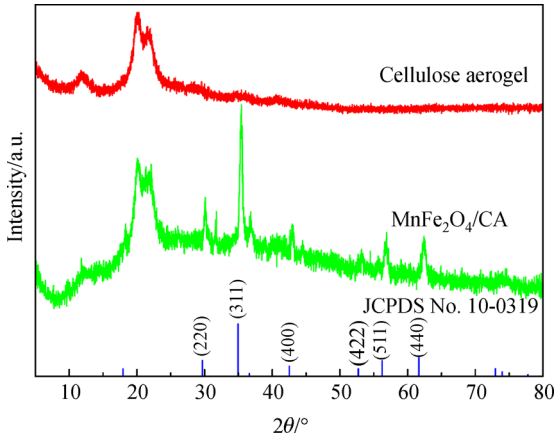

Fig. 2 XRD patterns of the cellulose aerogel and $MnFe_2O_4$/CA

indication of any other phases in the XRD pattern of $MnFe_2O_4$/CA.

The chemical states of elements in $MnFe_2O_4$/CA were investigated by XPS. The nanocomposite is composed of C, O, Mn and Fe, consistent with the results of EDX analysis. The photoelectron lines at around 284, 531, 642 and 711 eV (Fig. 3a) are attributed to C 1s, O 1s, Mn 2p and Fe 2p, respectively. Three different C 1s signals are observed at 284.8, 286.4 and 287.8 eV (Fig. 3b). The main peak at 284.6 eV is ascribed to the carbon atoms in C–C, C=C, and C–H bonds[18]. The other peaks at 286.4 eV, is assigned to the C–O, and the peak at 287.8 eV is attributed to the C=O bond[19]. The signals at 710.9 and 724.7 eV are related to the Fe $2p_{3/2}$ and Fe $2p_{1/2}$ (Fig. 3c), respectively, confirming the presence of Fe^{3+}[20]. The Mn $2p_{3/2}$ (Fig. 3d) signal appears at 641.6 eV, and the peak at 653.1 eV is ascribed to the Mn $2p_{1/2}$ signal, providing clear evidence for Mn^{2+} chemical state on the nanocomposite surface[21].

The loading content of $MnFe_2O_4$ in $MnFe_2O_4$/CA was measured by TG technique. As shown in Fig. 4a, the residual char yields above 800°C were 21.7% for the cellulose aerogel and 32.2% for $MnFe_2O_4$/CA, respectively. Thus, the content of $MnFe_2O_4$ can be roughly calculated as 10.5% in $MnFe_2O_4$/CA. In addition, it is seen in Fig. 4b that the room-temperature hysteresis curve of the nanocomposite shows the absence of hysteresis and coercivity, which is characteristic of superparamagnetic behavior[22]. The curve increases rapidly with increasing applied magnetic field, and exhibits saturation magnetization values of 7.7 $emu \cdot g^{-1}$.

The synthetic hybrid aerogel (i.e., $MnFe_2O_4$/CA) was verified to be a magnetically responsive material and actuator, as shown in Fig. 5. It can be tightly adhered to the surface of a magnet and maintain well-defined shape. Therefore, this class of aerogel with favorable shape stability and strong magnetic responsiveness may be used as a recyclable eco-friendly magnetically driven adsorbent for water purification, or a biodegradable electromagnetic device.

4 Conclusions

We demonstrate that the 3D architecture of cellulose aerogel can be used as a suitable eco-friendly template to encapsulate the superparamagnetic $MnFe_2O_4$ nanoparticles via a facile *in situ* chemical precipitation approach. The hexagonal $MnFe_2O_4$ nanoparticles have the sizes of 70 to 140 nm and were homogeneously immobilized in the cellulose aerogel. Moreover, the composite aerogel tightly

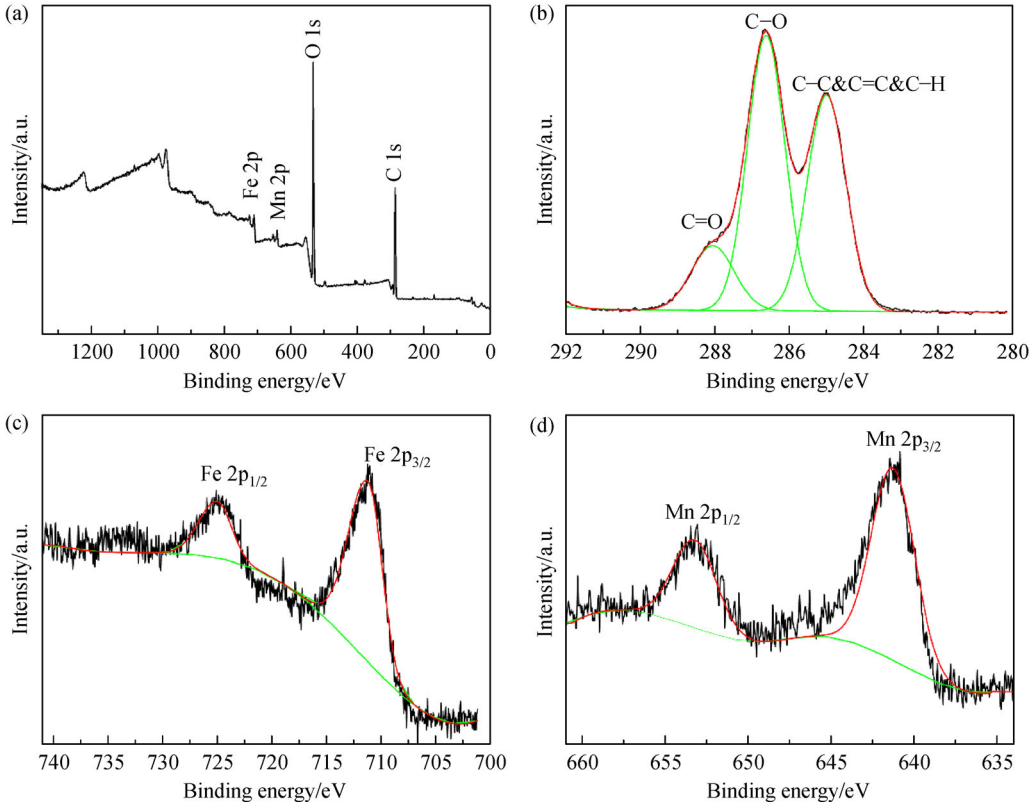

Fig. 3 Survey scan (a), O 1s (b), Fe 2p (c), and Mn 2p (d) XPS spectra of $MnFe_2O_4$/CA, respectively

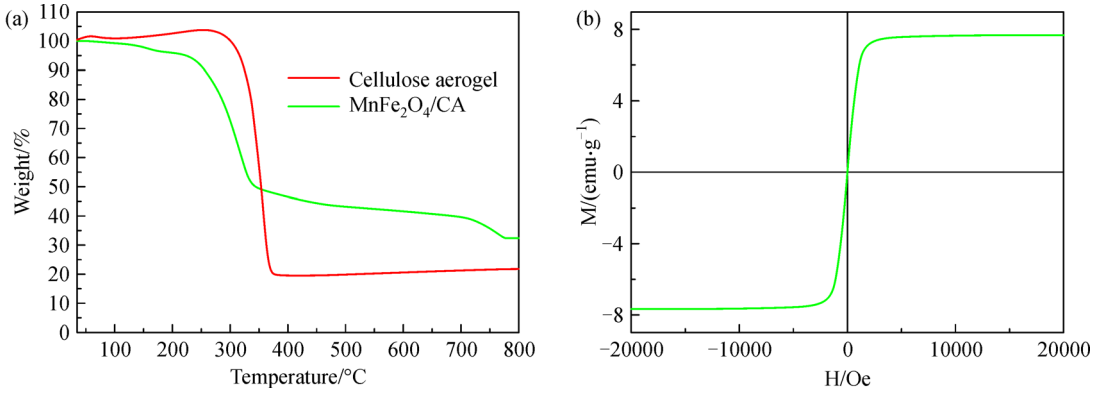

Fig. 4 (a) TG curves of the cellulose aerogel and $MnFe_2O_4$/CA; (b) hysteresis curve of $MnFe_2O_4$/CA.

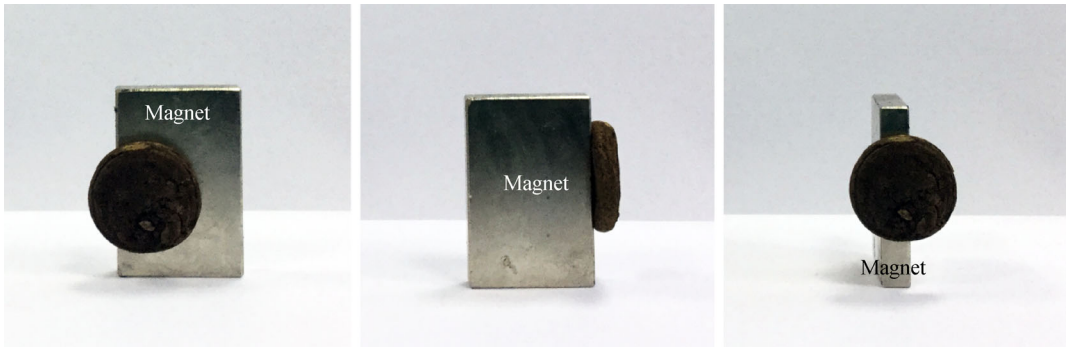

Fig. 5 Magnetic responsiveness of $MnFe_2O_4$/CA

adhered to the magnet surface, indicative of superior magnetic responsiveness. Therefore, this class of $MnFe_2O_4$/CA nanocomposite is expected to be useful as a kind of environmentally-friendly magnetically actuated adsorbent for the treatment of contaminated water.

Acknowledgements This study was supported by the National Natural Science Foundation of China (31270590, 31470584).

Compliance with ethics guidelines Jian Li, Yue Jiao, and Caichao Wan declare that they have no conflict of interest or financial conflicts to disclose.

This article does not contain any studies with human or animal subjects performed by any of the authors.

References

1. Sehaqui H, Zhou Q, Berglund L A. High-porosity aerogels of high specific surface area prepared from nanofibrillated cellulose (NFC). *Composites Science and Technology*, 2011, **71**(13): 1593–1599
2. Innerlohinger J, Weber H K, Kraft G. Aerocellulose: aerogels and aerogel-like materials made from cellulose. *Macromolecular Symposia*, 2006, **244**(1): 126–135
3. Pääkkö M, Vapaavuori J, Silvennoinen R, Kosonen H, Ankerfors M, Lindström T, Berglund L A, Ikkala O. Long and entangled native cellulose I nanofibers allow flexible aerogels and hierarchically porous templates for functionalities. *Soft Matter*, 2008, **4**(12): 2492–2499
4. Nguyen S T, Feng J, Ng S K, Wong J P W, Tan V B C, Duong H M. Advanced thermal insulation and absorption properties of recycled cellulose aerogels. *Colloids and Surfaces A: Physicochemical and Engineering Aspects*, 2014, **445**: 128–134
5. Xiong R, Lu C, Wang Y, Zhou Z, Zhang X. Nanofibrillated cellulose as the support and reductant for the facile synthesis of Fe_3O_4/Ag nanocomposites with catalytic and antibacterial activity. *Journal of Materials Chemistry A: Materials for Energy and Sustainability*, 2013, **1**(47): 14910–14918
6. Shi J, Lu L, Guo W, Zhang J, Cao Y. Heat insulation performance, mechanics and hydrophobic modification of cellulose-SiO_2 composite aerogels. *Carbohydrate Polymers*, 2013, **98**(1): 282–289
7. Leslie-Pelecky D L, Rieke R D. Magnetic properties of nanostructured materials. *Chemistry of Materials*, 1996, **8**(8): 1770–1783
8. Woo K, Hong J, Choi S, Lee H W, Ahn J P, Kim C S, Lee S W. Easy synthesis and magnetic properties of iron oxide nanoparticles. *Chemistry of Materials*, 2004, **16**(14): 2814–2818
9. Chin S F, Romainor A N B, Pang S C. Fabrication of hydrophobic and magnetic cellulose aerogel with high oil absorption capacity. *Materials Letters*, 2014, **115**: 241–243
10. Liu S, Yan Q, Tao D, Yu T, Liu X. Highly flexible magnetic composite aerogels prepared by using cellulose nanofibril networks as templates. *Carbohydrate Polymers*, 2012, **89**(2): 551–557
11. Wan C, Li J. Facile synthesis of well-dispersed superparamagnetic γ-Fe_2O_3 nanoparticles encapsulated in three-dimensional architectures of cellulose aerogels and their applications for Cr (VI) removal from contaminated water. *ACS Sustainable Chemistry & Engineering*, 2015, **3**(9): 2142–2152
12. Song Q, Zhang Z J. Controlled synthesis and magnetic properties of bimagnetic spinel ferrite $CoFe_2O_4$ and $MnFe_2O_4$ nanocrystals with core-shell architecture. *Journal of the American Chemical Society*, 2012, **134**(24): 10182–10190
13. Lee N, Hyeon T. Designed synthesis of uniformly sized iron oxide nanoparticles for efficient magnetic resonance imaging contrast agents. *Chemical Society Reviews*, 2012, **41**(7): 2575–2589
14. Lee J, Yang J, Ko H, Oh S, Kang J, Son J, Lee K, Lee S W, Yoon H G, Suh J S, Huh Y M, Haam S. Multifunctional magnetic gold nanocomposites: human epithelial cancer detection via magnetic resonance imaging and localized synchronous therapy. *Advanced Functional Materials*, 2008, **18**(2): 258–264
15. Li J, Wan C. Cellulose aerogels decorated with multi-walled carbon nanotubes: preparation, characterization, and application for electromagnetic interference shielding. *Frontiers of Agricultural Science and Engineering*, 2015, **2**(4): 341–346
16. Li J, Wan C, Lu Y, Sun Q. Fabrication of cellulose aerogel from wheat straw with strong absorptive capacity. *Frontiers of Agricultural Science and Engineering*, 2014, **1**(1): 46–52
17. Cai J, Kimura S, Wada M, Kuga S, Zhang L. Cellulose aerogels from aqueous alkali hydroxide-urea solution. *ChemSusChem*, 2008, **1**(1–2): 149–154
18. Gong W J, Tao H W, Zi G L, Yang X Y, Yan Y L, Li B, Wang J Q. Visible light photodegradation of dyes over mesoporous titania prepared by using chrome azurol S as template. *Research on Chemical Intermediates*, 2009, **35**(6): 751–760
19. Bose S, Kuila T, Uddin M E, Kim N H, Lau A K T, Lee J H. In-situ synthesis and characterization of electrically conductive polypyrrole/graphene nanocomposites. *Polymer*, 2010, **51**(25): 5921–5928
20. Yao Y, Cai Y, Lu F, Wei F, Wang X, Wang S. Magnetic recoverable $MnFe_2O_4$ and $MnFe_2O_4$-graphene hybrid as heterogeneous catalysts of peroxymonosulfate activation for efficient degradation of aqueous organic pollutants. *Journal of Hazardous Materials*, 2014, **270**: 61–70
21. Fu Y, Xiong P, Chen H, Sun X, Wang X. High photocatalytic activity of magnetically separable manganese ferrite–graphene heteroarchitectures. *Industrial & Engineering Chemistry Research*, 2012, **51**(2): 725–731
22. Esmaeili A, Ghobadianpour S. Vancomycin loaded superparamagnetic $MnFe_2O_4$ nanoparticles coated with PEGylated chitosan to enhance antibacterial activity. *International Journal of Pharmaceutics*, 2016, **501**(1–2): 326–330